

Development of an *in situ* calibration method for current-to-voltage converters for high-accuracy SI-traceable low dc current measurements

This content has been downloaded from IOPscience. Please scroll down to see the full text.

2013 Metrologia 50 509

(<http://iopscience.iop.org/0026-1394/50/5/509>)

View [the table of contents for this issue](#), or go to the [journal homepage](#) for more

Download details:

IP Address: 132.203.227.62

This content was downloaded on 04/03/2015 at 19:27

Please note that [terms and conditions apply](#).

Development of an *in situ* calibration method for current-to-voltage converters for high-accuracy SI-traceable low dc current measurements

George P Eppeldauer, Howard W Yoon, Dean G Jarrett and Thomas C Larason

National Institute of Standards and Technology, Gaithersburg, MD, USA

Received 21 May 2013, in final form 5 August 2013

Published 20 September 2013

Online at stacks.iop.org/Met/50/509

Abstract

For photocurrent measurements with low uncertainties, wide dynamic range reference current-to-voltage converters and a new converter calibration method have been developed at the National Institute of Standards and Technology (NIST). The high-feedback resistors of a reference converter were *in situ* calibrated on a high-resistivity, printed circuit board placed in an electrically shielded box electrically isolated from the operational amplifier using jumpers. The feedback resistors, prior to their installation, were characterized, selected and heat treated. The circuit board was cleaned with solvents, and the *in situ* resistors were calibrated using measurement systems for 10 k Ω to 10 G Ω standard resistors. We demonstrate that dc currents from 1 nA to 100 μ A can be measured with uncertainties of 55×10^{-6} ($k = 2$) or lower, which are lower in uncertainties than any commercial device by factors of 10 to 30 at the same current setting. The internal (NIST) validations of the reference converter are described.

(Some figures may appear in colour only in the online journal)

1. Introduction

In modern radiometry, for photometric units such as the candela and for radiometric units such as power, radiance or irradiance, the units are derived from the cryogenic, electrical-substitution radiometer (ESR) [1, 2]. The ESR determines the optical power of the radiation by comparison with the equivalent temperature rise in the receiving cavity produced by the electrical power, and thus, the optical watt is made traceable to the electrical watt. Since the ESR is difficult to use and not easily transported, the optical power responsivity is transferred to photodiodes by substitution calibrations. These photodiodes are operated in photovoltaic mode and their photocurrents are measured. These photodiodes are calibrated for optical power responsivity, which has the units of A W^{-1} , and the photocurrent should be linearly proportional to the incident optical power. Since most photometers and radiometers are operated in photovoltaic mode, photocurrent measurement with the lowest possible uncertainty is critical, and the current measuring device must have an uncertainty budget with the

measurements made traceable to *Le Système international d'unités* (SI). The need for accurate low-current measurements also exists in other fields such as medical dosimetry, testing for material purity, particulate measurement and charge mobility.

Typically, commercial low-current sources or meters are calibrated in two different ways. In the first calibration method, low dc currents are generated by charging different air capacitors with a linearly varying voltage ramp. For this current source, the voltage ramp and its slope must be stable, but the dielectric absorption and leakage resistance of the capacitor can cause non-linearity in the voltage ramp. The obtained absolute current can be used to calibrate low-current meters. A calibration setup using this method was built and reported for the calibration of picoammeters [3]. Using offset current compensation and also a galvanic (opto-coupling) isolation between the computer and the ramp generator, a current calibration uncertainty of 30×10^{-6} ($k = 1$) was reported at an output current of 10 pA. This uncertainty increased to 6% ($k = 1$) at 1 fA. This absolute current source was not utilized for photodiode output current calibrations.

In the second, more common, calibration method, the currents are converted to voltages using standard resistors. These standard resistors can be calibrated at the national labs either individually or in resistor boxes but the user must be able to set up a low-noise circuit utilizing these resistors. The currents then can be determined using Ohm's law, $V = I \times R$. The voltage can be routinely measured but the uncertainty of the current-to-voltage conversion must be known for both setups with the current source and thereafter for the photodiode that replaces the current source. The output resistance of the current source and also the shunt resistance of the photodiode have major influences on the amplification of the input noise and drift of the current-to-voltage converter [4]. A high (known) constant voltage was converted into low currents with high-value standard resistors. A test current-to-voltage converter was used to measure the low currents [5]. This photocurrent-to-voltage converter calibration method resulted in expanded uncertainties of 0.38% ($k = 2$) at 1 pA and 0.046% ($k = 2$) at 10 pA. The calibration uncertainty was dominated by two dominant uncertainty components: the voltage dependence and stability of the 10 G Ω to 100 T Ω standard resistors and the $1/f$ noise from the converter.

2. Motivation

Traditional transimpedance gain calibrations, using external standard resistors, have limitations. Generally, the reference resistors are used to determine the current from a variable-output current source from a measurement of the voltage drop across the resistor. In our first-generation work, commercially available precision resistors were used as reference resistors to calibrate an operational-amplifier-based current-to-voltage converter. In this first attempt, the reference resistors were connected in series to the converter input to transfer the converter from current measurement mode into voltage measurement mode. In this case, the unknown feedback resistance of the operational amplifier (OA) is determined from the measured voltage amplification, which depends on the reference resistor and the feedback resistance. Here, both the input and the output voltages can be measured with low uncertainty. In the other application, the reference resistors (up to $10^8 \Omega$) were used to measure the current from a stable current source. With both methods, because of the use of external reference resistors, the converter output noise is large especially at high signal gains. The expanded uncertainty obtained at the calibration of the 10^9 V A^{-1} gain of the test converter was 0.03% ($k = 2$). When the test converter gain was increased to 10^{10} V A^{-1} , the input current had to be decreased by a decade to be able to calibrate this gain. At this current, the small (50 mV) voltage drop on the $10^8 \Omega$ reference resistor had a 0.75% fluctuation. Instead of propagating this uncertainty to the 10^{10} V A^{-1} gain of the test converter, the 10^{10} V A^{-1} gain was calibrated against the neighbouring 10^9 V A^{-1} gain and a 0.035% ($k = 2$) expanded uncertainty could be obtained. Instead of the external resistor method, a better method had to be developed with a significantly improved signal-to-noise ratio in the current measurement.

One of the main lessons learned from the results of the published methods and from our previous, initial

current-to-voltage converter calibrations is that the high-value reference resistors must be electrically shielded during the gain calibrations of the converter to minimize noise pickup, and also calibrated as a system to reduce the transfer uncertainties. The simplest way to achieve both of these goals was to place the calibrated resistors on a high-resistivity circuit board inside an electrically shielded box, which could be directly used as a current-to-voltage converter. Since the converter does not require serial resistors (connected to its input) the calibrated resistors can be used directly as feedback resistors.

The signal-conversion uncertainties could be improved in our second-generation calibrations, [6] where a reference current-to-voltage converter was developed using internal (electrically shielded by the converter box) reference feedback resistors. The decade feedback resistors (from $10^4 \Omega$ to $10^8 \Omega$) were calibrated against the National Institute of Standards and Technology (NIST) standard resistors. With this design, the noise pickup was significantly decreased. This second-generation work was focused on the signal-conversion scale realization and its propagation to applications. The expanded uncertainty of the input current measurement at gain 10^8 V A^{-1} was 0.012% ($k = 2$). The reference signal-conversion scale (implemented by the converter standard) could be transferred to different radiometric and photometric calibrations. Test converters using feedback resistors up to $10^{10} \Omega$ were calibrated against the reference converter using direct converter substitution. The expanded uncertainty obtained at gain 10^{10} V A^{-1} was 0.013% ($k = 2$). In this work, the shunt resistance requirements for the photodiodes (that substitute the dc current source) were also discussed to obtain similar uncertainties in both photodiode measurements and electrical calibrations. In addition to dc current measurements, the current-to-voltage converter calibration method was extended to ac.

In our third-generation calibrations, as described in this paper, the previous calibration method [6] has been further improved. The resistances of the feedback resistors up to $10^{10} \Omega$ are measured *in situ*, together with the parallel resistances of the circuit board, rotary-gain switch and feedback capacitors. The reference standards for these calibrations and the resistance elements of the converters are both improved. The resistance measurements are made traceable to low-uncertainty $10^9 \Omega$ and $10^{10} \Omega$ resistors, which have been recently developed by the NIST Quantum Measurement Division [7]. The selection criteria of the seven feedback resistors, the design considerations of the improved current-to-voltage converter and the calibration procedure of the feedback components are described. The current-to-voltage conversion uncertainties are determined.

3. Reference current-to-voltage converter design

The circuit diagram of the reference current-to-voltage converter is shown in figure 1. The feedback components are $R1 = 10^4 \Omega$, $R2 = 10^5 \Omega$, $R3 = 10^6 \Omega$, $R4 = 10^7 \Omega$, $R5 = 10^8 \Omega$, $R6 = 10^9 \Omega$; $R7 = 10^{10} \Omega$, $C1 = C2 = 6.8 \text{ nF}$, $C3 = 1500 \text{ pF}$, $C4 = 150 \text{ pF}$ and $C5 = 15 \text{ pF}$. The capacitance values were chosen to obtain about 100 Hz (3 dB)

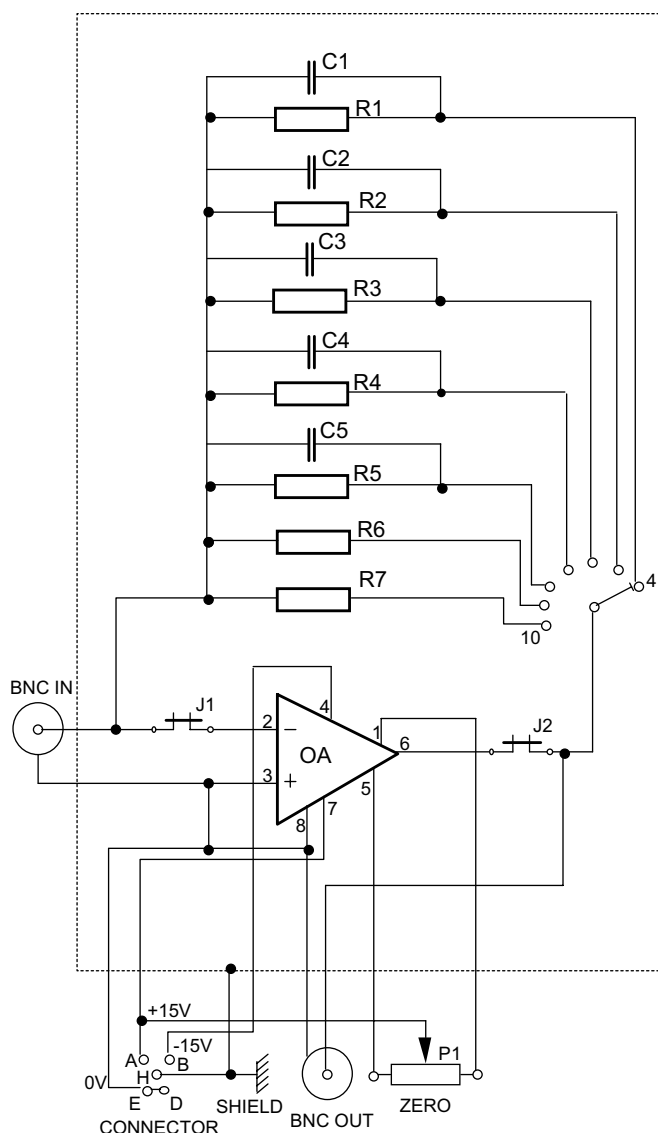


Figure 1. Circuit diagram of the third-generation reference I - V converter.

upper roll-off frequencies. The components are soldered onto a printed circuit board (PCB) using Rogers 4003C material with a minimum surface resistivity of $4.2 \times 10^{15} \Omega$ and a minimum volume resistivity of $1.7 \times 10^{16} \Omega \text{ cm}$. The board is mounted in an electrically shielded aluminum box to avoid 60 Hz and noise pickup by the high-resistance components. Since the gain switch, the feedback resistors and capacitors, and the PCB are electrically connected to the OA between its input and output, the resistors are calibrated with all the above components included in the resistance calibrations. The OA also remains in place but the two gold-pin jumpers, J1 and J2, built into the circuit board at the OA input and output are removed to isolate the OA when the resistances are measured. To minimize the parallel resistances, a rotary switch with insulation resistances $>4 \times 10^{14} \Omega$ was selected from several different commercially available models. Solder mask was not used on the board to avoid degradation of the board insulation resistance. In order to minimize shunt effects of remaining leakage currents, a large size board was used with increased separations between the

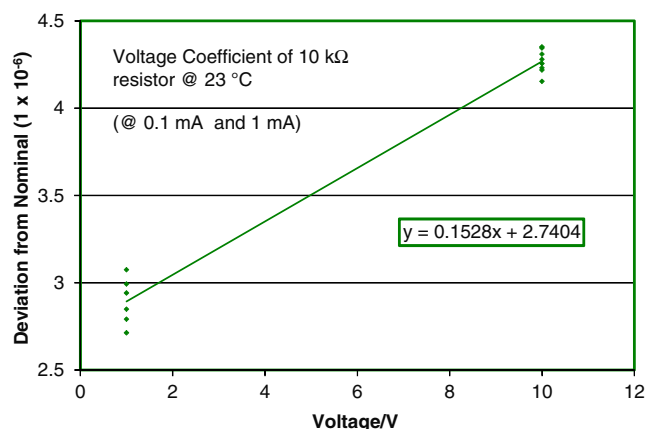


Figure 2. Deviation from nominal value of a $10 \text{ k}\Omega$ resistor from measurements at 1 V (0.1 mA) and 10 V (1 mA) at 23°C .

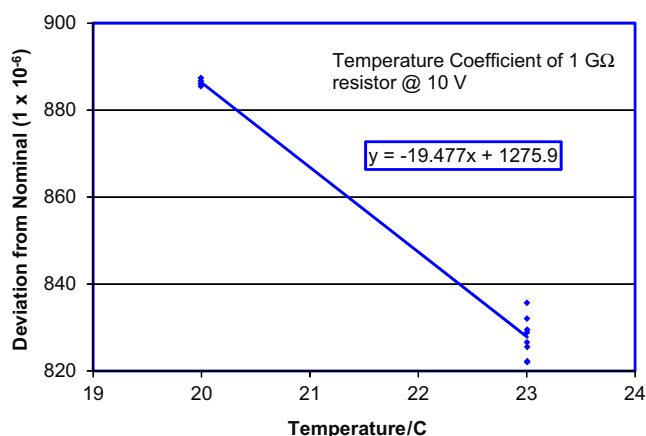


Figure 3. Deviation from nominal value of a $1 \text{ G}\Omega$ resistor with a temperature change from 20°C to 23°C at 10 V.

metal traces and components. Additional guarding for further decreasing the shunt effects was not needed.

4. Feedback resistor selections

Precious metal oxide (PMO) film type resistors were selected for use as feedback resistors. A heat-treatment process developed for the NIST high-resistance standards has been used to treat the $1 \text{ G}\Omega$ and $10 \text{ G}\Omega$ resistance elements used in the feedback circuit. Groups of resistance elements were measured prior to the heat treatment to select those closest to the nominal value, and then the elements were heat treated at 65°C for 250 h to accelerate the ageing and to improve the long-term stability. The temperature coefficient of resistance (TCR), the voltage coefficient of resistance (VCR), drift and settling time measurements were made following the heat treatment to select the most stable and closest to nominal value resistance elements to be used in the reference converter.

As an example, figure 2 shows a voltage coefficient of $0.153 \times 10^{-6} \text{ V}^{-1}$ for a $10 \text{ k}\Omega$ resistance element at 23°C . Figure 3 shows a temperature coefficient of $-19.5 \times 10^{-6} \text{ }^\circ \text{C}^{-1}$ for a $1 \text{ G}\Omega$ resistance element at 10 V.

After soldering the resistors to the PCB, the measurements were repeated. The final measurements were made with a dual-source bridge [8].

Table 1. Results of the feedback resistance calibrations (at 23.0 °C).

Resistor	Nominal value/ Ω	Correction (10^{-6})	Uncertainty (10^{-6})	Calibration voltage/V	Temperature coeff./($10^{-6} \text{ } ^\circ\text{C}^{-1}$)	Voltage coeff./(10^{-6} V^{-1})	Load coeff.
R1	1×10^4	4.3	0.3	10 @ 1 mA	4.0	0.15	Yes
R2	1×10^5	50.1	0.8	10	4.1	Unknown	n/a
R3	1×10^6	27.1	0.8	10	1.9	Unknown	n/a
R4	1×10^7	103	6	10	0.8	0.003	n/a
R5	1×10^8	12	6	10	0.8	0.008	n/a
R6	1×10^9	829	18	10	-19.5	-0.17	n/a
R7	1×10^{10}	12	50	10	-8.2	0.007	n/a

5. Feedback resistor calibrations

The calibration of a standard resistor requires a defined set of terminals and a screened enclosure that serves as a Faraday cage. The calibration of standard resistors embedded in instrumentation and circuits is challenging and is typically not done with the same level of accuracy as a standard resistor with well-defined terminals. The approach taken here was to design the current-to-voltage amplifier circuit such that the standard resistors could be calibrated *in situ* with the calibration including the standard resistor and other components that form the scaling ratio with the OA. During calibration, the OA is isolated from the other components and the amplifier circuit input/output terminals are used as the resistor terminals. The resistors, capacitors, circuit board, rotary switch, input/output connectors and shielded case are treated as standard resistors and calibrated using the same measurement systems as those used for a traditional standard resistor. The calibration of the on-board standard resistors may be repeated at regular intervals to establish long-term drift rates. NIST standard resistor calibration systems were used in the preliminary testing, demonstrating that the capacitors negligibly affect the calibration of the standard resistors [9].

The conditions and results of the feedback resistance calibrations are summarized in table 1. The resistors were selected so that their nominal values changed between 10 k Ω and 10 G Ω in decade steps. The temperature coefficients, the voltage coefficients and the load coefficients of the measured resistance together with the relative expanded uncertainty of the measurement in 10^{-6} are included in table 1. The expanded uncertainty from 0.3×10^{-6} ($k = 2$) at 10 k Ω gradually increases to 50×10^{-6} ($k = 2$) at 10 G Ω . The resistance corrections to obtain the decade nominal values are also included in the table. The calibration temperature was regulated at 23.0 °C.

6. Resistor installation onto the PCB

Figure 4 shows the effect of the PCB contamination and cleaning on the calibration of the 10 G Ω resistor. The resistance elements (10 k Ω to 10 G Ω) were calibrated prior to being soldered onto the PCB. Prior to being soldered to the PCB, the 10 G Ω resistance element was calibrated and had a correction from nominal of 25×10^{-6} as shown in the upper left area of figure 4. After the 10 G Ω resistor was soldered to the PCB and measured *in situ*, that measurement

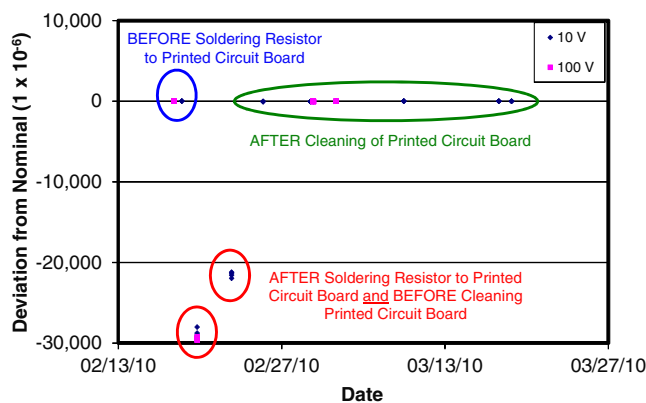


Figure 4. PCB cleaning effect on the 10 G Ω feedback resistance calibration.

indicated that the resistor had a correction from nominal of $-25\,000 \times 10^{-6}$, as shown on the lower left of figure 4. This change would require a resistance of 400 G Ω to be in parallel with the resistance element. The PCB material itself was orders of magnitude higher in resistance than 400 G Ω , which indicated some contamination of the PCB surfaces. Several cleanings of the PCB surfaces were able to remove contamination and yielded a series of *in situ* measurements of the 10 G Ω resistor within 10×10^{-6} of the resistor calibration prior to soldering to the PCB shown on the upper right of figure 4. The measurements shown in figure 4 were made at both 10 V and 100 V.

7. DC input current and signal-gain calibrations

The calibrated transimpedance amplifier must be used with a stable, variable-current source so that other current preamplifiers and electrometers can then be calibrated using the current source. The current from a variable-output dc current source is measured with the reference current-to-voltage converter. Here we describe the current circuit for this transfer and the issues in obtaining the lowest uncertainty transfers using such a circuit. Figure 5 shows the scheme of the substitution-type current-to-voltage converter calibration. The current I from the current source is

$$I = \frac{V_1(I) - V_1(I = 0)}{R} \quad (1)$$

where $V_1(I = 0)$ is the converter output voltage for $I = 0$ and R is the feedback resistor of the OA in the converter. The

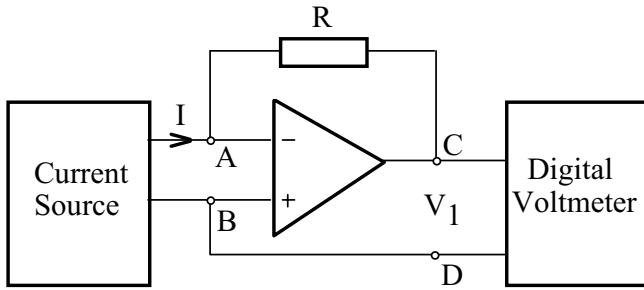


Figure 5. Current determination with the reference I - V converter.

voltage subtraction cancels the output offset voltage of the reference current-to-voltage converter. After calibrating the dc current from the current source (with the reference converter), the signal gain of test converters can be determined. The test converter can be substituted for the reference converter. Its output voltage will be V_2 . The signal gain (G_S) of the test converter will be

$$G_S = \frac{V_2(I) - V_2(I = 0)}{I} \quad (2)$$

where $V_2(I)$ is the test converter output voltage for input current I , $V_2(I = 0)$ is the test converter output voltage for $I = 0$, and I is the current as determined by equation (1). The output offset voltage of the test converter is cancelled out by the voltage subtraction in equation (2).

In a simple conversion when a small load resistor (without an OA) converts a large current into a voltage, the conversion uncertainty can be low. In the case of small photocurrent measurements, when an OA-based current-to-voltage converter is used with high-value feedback resistors, the conversion uncertainty can be low only if the loop gain of the converter is high. Ignoring the ideal diode and the parasitic series resistance in the photodiode model [10], the signal gain (G_S) of a current-to-voltage converter in dc measurement mode is [4]

$$G_S = R \frac{1}{1 + G_L^{-1}} \quad (3)$$

where R is the feedback resistor of the OA of the converter and G_L is the loop gain of the analogue control loop in the converter:

$$G_L = A_0 \beta_0 = A_0 \frac{R_S}{R_S + R} \quad (4)$$

where A_0 is the dc open-loop gain of the OA used in the converter and β_0 is the feedback attenuation, where R_S is the shunt resistance of the photodiode attached to the input of the converter (at applications). For $A_0 = 10^6$, when using an $R = 1 \text{ G}\Omega$ feedback resistor, the shunt resistance of the attached photodiode must be equal to or higher than $R_S = 10^8 \Omega$ if a conversion expanded uncertainty of about 0.001% (equal to 10×10^{-6}) ($k = 2$) is required. Similarly, at calibration, the output resistance of the current source (attached to the input of the converter) will substitute for the photodiode shunt resistance (R_S) in equation (4). Again, this resistance must be higher than $10^8 \Omega$. In our case, the

output resistance of the current source (Keithley 6430) at 1 nA was $10^{12} \Omega$, which made the conversion uncertainty negligibly small during the calibration. This issue of output resistance dependence is further discussed later in the paper. Using photodiodes with $\text{G}\Omega$ level shunt resistances, the uncertainty component produced by the output noise and drift can be minimized. In this case, the overall uncertainty of a photocurrent measurement can be dominated by the uncertainty component produced by the *in situ* feedback resistance calibration(s).

8. Validation and intercomparison

Initially, the NIST-developed converters were tested using a commercial current source, and the measured currents compared with the stated currents from the current source. The comparison results of dc current calibrations performed with a commercial (Keithley 6430) instrument, the previous NIST reference converter (labelled ADS) and the currently discussed NIST reference converter (labelled SDX) are shown in figure 6. The relative expanded uncertainty of the high-quality commercial current source (shown with triangles \blacktriangle) was close to 0.1% ($k = 2$) between 10^5 V A^{-1} and 10^{10} V A^{-1} . The differences from the Keithley 6430 current source measurements are shown with closed diamonds (\blacklozenge) relative to the ADS reference converter and with open squares (\square) relative to the SDX reference converter measurements. The differences between the measured currents and the stated currents of the Keithley source were in agreement within the expanded uncertainties ($k = 2$). The uncertainty of the current as measured by the ADS converter was 0.012% ($k = 2$) using the $10^8 \Omega$ highest calibrated feedback resistor of this converter. The current measurement uncertainty obtained with the SDX converter was 55×10^{-6} ($k = 2$) at gain 10^9 V A^{-1} (also shown in table 2). Figure 6 also shows that the current measurement uncertainty of the SDX converter increases to 62×10^{-6} at the 10^{10} V A^{-1} gain. The dominant reason for this uncertainty increase is the 2.8 times higher feedback resistance uncertainty at the 10^{10} V A^{-1} gain compared with the feedback resistance uncertainty at the 10^9 V A^{-1} gain. The uncertainty improvement with the SDX reference converter is about $1\frac{1}{2}$ decades. It can also be seen in figure 6 that the first- and second-generation reference converters measure within their reported uncertainties at the signal gains where their feedback resistors were calibrated. This is a validation of the NIST-developed reference current-to-voltage converters.

The uncertainty budget of dc current measurement for all signal gains of the third-generation (SDX) converter is shown in table 2. As shown in table 1, the expanded uncertainty ($k = 2$) of the feedback resistance calibration strongly depends on the nominal value of the resistance. This type-B uncertainty and the type-A uncertainty produced by the output noise and drift can dominate the combined standard uncertainty of the input current measurements. At the highest, 10^{10} V A^{-1} gain of the converter, the dominant uncertainty component (shown in table 2) originates from the 25×10^{-6} ($k = 1$) relative standard uncertainty of the $10 \text{ G}\Omega$ feedback resistance calibration. According to equation (4), the loop

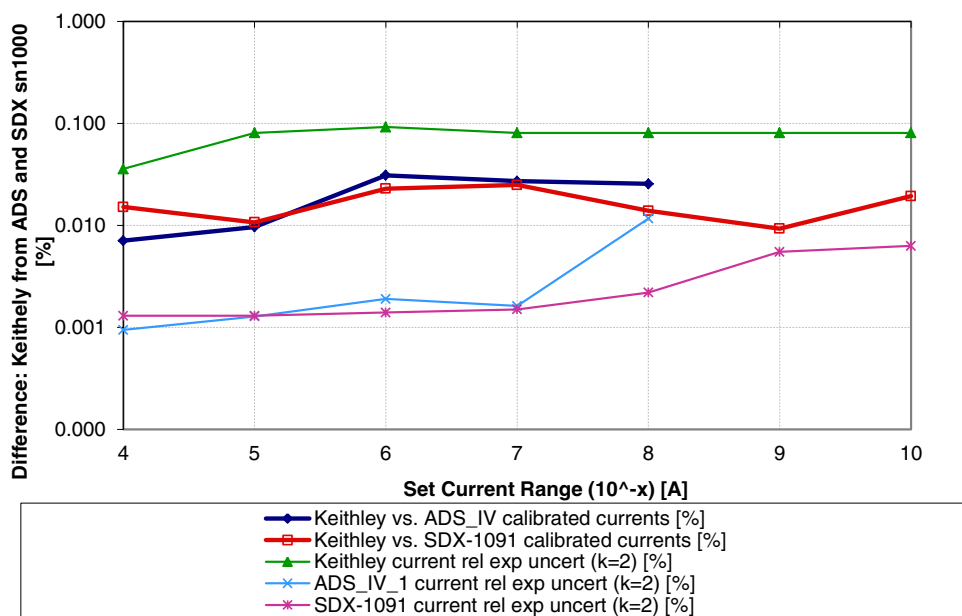


Figure 6. Comparison of the dc current measurements using a commercial (Keithley 6430) instrument to the current measured with the second-generation (ADS) and third-generation (SDX) reference converters. The differences in the expanded uncertainties ($k = 2$) comparing the second- and third-generation I - V converters with the commercial source are plotted as a function of current range.

Table 2. Uncertainty budget of dc current measurement with the third-generation reference current-to-voltage (SDX) converter at all its signal gains using the Keithley 6430 current source.

Uncertainty components	Type	Relative uncertainty (1×10^{-6})						
		10^4 V A^{-1}	10^5 V A^{-1}	10^6 V A^{-1}	10^7 V A^{-1}	10^8 V A^{-1}	10^9 V A^{-1}	10^{10} V A^{-1}
Feedback resistance	B	0.2	0.4	0.4	3	3	9	25
Resistance correction for application temperature change of 1 °C	A	4	4.1	1.9	0.8	0.8	19.5	8.2
Short-term instability of input current I	A	1	1	1	1	1	6	6
V_1 voltage measurement (HP DVM 3458 A)	B	2	2	2	2	2	2	2
Output noise and drift (4 days)	A	4	4	6	6	10	16	16
Loop gain	A	2	2	2	2	2	2	2
Non-linearity of the SDX converter	B	2	2	2	2	2	2	2
Combined standard uncert. of I meas.		6.7	6.8	7.3	7.7	11	27.7	31.6
Expanded total uncert. ($k = 2$) of I meas.		13	14	15	15	22	55	63

gain related uncertainty component will not change because the R feedback resistances are much smaller for all signal-gain selections than the output resistance of the Keithley 6430 current source. The output resistance changes from $10^{12} \Omega$ at 1 nA (used at the 10^9 V A^{-1} and 10^{10} V A^{-1} gain selections) to $10^7 \Omega$ at 100 μA (used at the 10^4 V A^{-1} and 10^5 V A^{-1} gain selections). The four-day output noise and drift will not change for the 10^{10} V A^{-1} gain compared with the 10^9 V A^{-1} gain because the amplification (inverse of the feedback attenuation) for the input noise and drift will not change significantly. The expanded total uncertainty of 63×10^{-6} ($k = 2$) was estimated for the measurement of 1 nA dc input current at the 10^{10} V A^{-1} signal gain of the third-generation reference current-to-voltage converter. Measuring the same input current at the 10^9 V A^{-1} gain, the current measurement uncertainty

decreased to 55×10^{-6} ($k = 2$). At this gain, the input current can be increased to 10 nA, resulting in somewhat decreased noise and drift. In the described measurements, the overall input current range was six decades (from 10^{-9} A to 10^{-4} A). The 1 nA limit was produced by the current uncertainty of the source.

Since the uncertainties of the Keithley current source were not sufficiently low to test the NIST converter, the calibrated R_r resistance ratios of the neighbouring gains were checked to determine the agreement with the measured V_r voltage ratios:

$$R_r \text{ versus } V_r = \frac{\frac{R_{n+1}}{R_n} - \frac{V_{n+1}}{V_n}}{\frac{V_{n+1}}{V_n}} \quad (5)$$

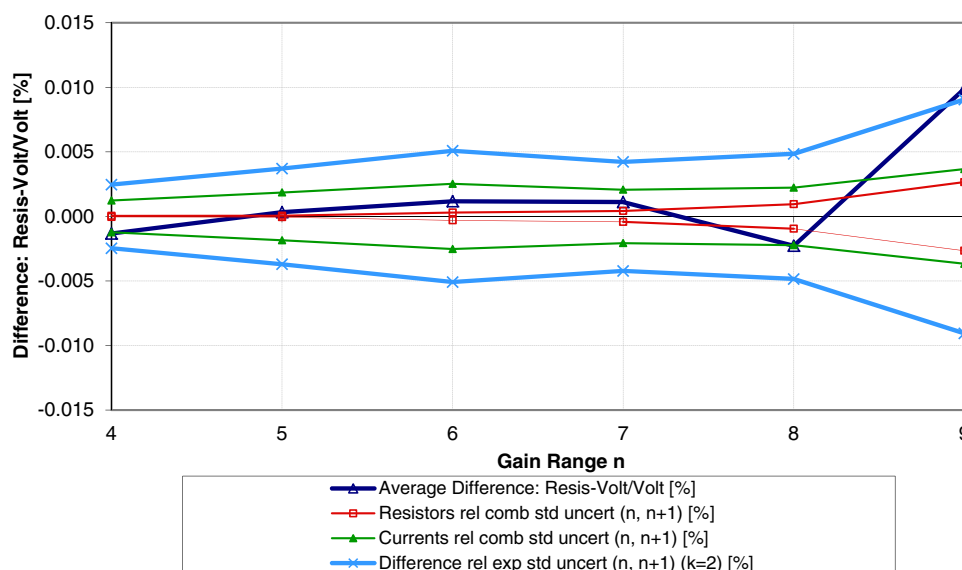


Figure 7. Results of resistance ratio versus output voltage ratio comparison for the third-generation reference converter. The resistance, current and ratio-difference uncertainties are shown as well.

where the neighbouring (calibrated) feedback resistor ratios are R_{n+1}/R_n , and the (measured) output voltage ratios for the ranges that use these resistors are V_{n+1}/V_n . The average differences of the ratios in equation (5) are shown in figure 7 in per cent at the 10^4 V A^{-1} to 10^9 V A^{-1} gains of the reference converter. The graph shows with open triangles (Δ) the average differences of three scans comparing the ratios of neighbouring calibrated resistances to the measured output voltage ratios. The ratios at gains 10^4 V A^{-1} to 10^8 V A^{-1} agree to better than 0.0022% (22×10^{-6}). This verifies that the I - V conversion (or signal gain) determination (and uncertainty) tracks together with the resistances (and resistance uncertainties) at these signal gains of the reference converter. The graph illustrates that the tracking is better than 0.01% up to gain range 9 (10^9 V A^{-1}). The graph also shows with open squares the relative combined standard uncertainties of the calibrated resistances. The full triangles (\blacktriangle) show the relative combined standard uncertainty of the dc current measurements. The cross-markers (\times) show the relative expanded standard uncertainties of the ratio differences.

Test current-to-voltage converters can be calibrated against the reference current-to-voltage converter using converter substitution. The error budget of the signal-gain determination of a test converter at its 10^{10} V A^{-1} gain is shown in table 3. The current measurement was performed with the third-generation SDX reference converter at 10^9 V A^{-1} gain. The expanded total uncertainty of the signal gain, G_S , is 65×10^{-6} ($k = 2$). This uncertainty would increase to 72×10^{-6} if the 10^{10} V A^{-1} gain of the reference converter were used (instead of the 10^9 V A^{-1} gain). The reason for this uncertainty increase is the 2.8 times higher uncertainty in the resistance measurement of the $10 \text{ G}\Omega$ feedback resistor. In situations like this, instead of matching the signal gain of the reference converter to the gain (being calibrated) of the test converter, the one decade lower signal gain of the reference converter could be used.

Table 3. Uncertainty budget of the signal-gain determination of a test current-to-voltage converter at its 10^{10} V A^{-1} signal gain using the Keithley 6430 current source calibrated at the 10^9 V A^{-1} gain of the SDX reference converter.

Uncertainty components at 10^{10} V A^{-1} signal gain	Type	Relative uncertainty ($\times 10^{-6}$)
I measurement	B	27.7
Short-term instability of input current I	A	6
V_2 voltage measurement (HP DVM, 3458 A)	B	2
Output noise and drift (4 days)	A	16
Loop gain	A	2
Combined standard uncertainty ($k = 1$) of signal gain G_S		32.6
Expanded total uncertainty ($k = 2$) of signal gain G_S		65

As shown in table 2, the uncertainties at low signal-gain calibrations are significantly lower than at high signal gains. In this table, the uncertainty budget of dc current measurements for all signal gains of the third-generation (SDX) reference converter is shown when the output current from a Keithley 6430 source is measured. During the dc current calibrations when the signal gains are decreased in decade steps, the current from the current source is also increased in decade steps. While the output resistance of the Keithley 6430 current source (using the 1 nA output current range) was $10^{12} \Omega$ at the 10^9 V A^{-1} and 10^{10} V A^{-1} gain selections of the converter, the output resistance decreased to $10^7 \Omega$ at the 10^4 V A^{-1} (lowest converter gain) where the highest source current of $100 \mu\text{A}$ was measured. Since the output resistance of the source, for all signal-gain selections of the converter, was much higher than the feedback resistance of the converter, the noise and drift amplifications, as shown in equation (4), were minimized.

Different dc current sources may have different output resistances. For example, the output resistance of the Keithley

Table 4. Changes in the noise amplification ($1/\beta_O$) of a current-to-voltage converter at gains 10^9 V A^{-1} and 10^8 V A^{-1} versus the output resistance R_{out} of current source(s) at 10 nA output current.

	Feedback resistance, R/Ω									
	10^9					10^8				
R_{out}/Ω	10^{12}	10^{11}	10^{10}	10^9	10^8	10^7	10^9	10^8	10^7	10^6
$1/\beta_O$	1.001	1.01	1.1	2	11	101	1.1	2	11	101

263 source is $10^9 \Omega$ at 1 nA (using the lowest, 2 nA full-scale range) and $10^8 \Omega$ at 10 nA (using the 20 nA full-scale range). For both current settings the output resistance is lower than the 2 G Ω to 5 G Ω shunt resistance of a high-quality Si photodiode. As an example, table 4 shows how the noise and drift amplification $1/\beta_O$ (the inverse feedback attenuation in equation (4)) changes for the output of a current-to-voltage converter versus the output resistance of a current source(s) at two feedback resistances ($10^9 \Omega$ and $10^8 \Omega$) of the converter. The table shows that the noise gain at 10 nA source output current increases from 1.01 ($R = 10^9 \Omega$ and $R_{\text{out}} = 10^{11} \Omega$) to 11 ($R = 10^9 \Omega$ and $R_{\text{out}} = 10^8 \Omega$) if the Model 6430 source is replaced by the Model 263 source. This one decade increase in the noise amplification will increase the 16×10^{-6} dominating uncertainty component in table 2 (at the 10^9 V A^{-1} gain) to 160×10^{-6} , resulting in 320×10^{-6} ($k = 2$) current measurement uncertainty instead of the previous 40×10^{-6} ($k = 2$) (using the Model 6430). Accordingly, the 100 M Ω output resistance (in the 20 nA range) should not be used to avoid increased amplification (a decade higher than in the 2 nA range) for noise and drift.

The output resistances of the Keithley 2400 and 6430 current sources are equal in the 1 μA to 100 mA current ranges: $10^{12} \Omega$ at 1 μA , $2 \times 10^{11} \Omega$ at 10 μA and $2 \times 10^{10} \Omega$ at 100 μA . All of these output resistances are much higher than the shunt resistance ($\sim 5 \text{ G}\Omega$) of a high-quality Si photodiode, resulting in low noise amplification for the converter outputs. While the lowest current range of the Model 2400 source is 1 μA , the lowest range of the Model 6430 source is 1 pA. The manufacturer-reported current accuracy in the 1 μA full-scale range is 0.035% for Model 2400 and 0.05% for Model 6430. However, for Model 6430, the reported accuracy remains 0.05% down to the 1 nA range and then the accuracy increases to 0.15% at 100 pA and to 1% at 1 pA. These accuracy values can be used as relative expanded uncertainties ($k = 2$). In order to avoid an increase in the signal-gain calibration uncertainties, in the measurements described here, the lowest set current of Model 6430 was 1 nA. No accuracy specifications are reported for the Model 2400 current source below 1 μA . The low signal-gain uncertainty of the SDX reference converter could be utilized for dc current measurements lower than 1 nA (100 pA or 10 pA) with current sources where the current uncertainty was not (significantly) increased in these current range(s).

The converter signal-gain calibrations and the real photocurrent measurements (from a photodiode) should be performed with similar electrical characteristics. This means that the photodiode shunt resistance must be in the 2 G Ω

to 5 G Ω (or higher) range [4] to minimize the reciprocal of the feedback attenuation (equal to the amplification) in equation (4). For calibrations, the output resistance of the current source should also be high (a few G Ω or higher) to keep the amplification for the input noise and drift of the converter-amplifier low. For smaller source output resistances or photodiode shunt resistances, the measurement uncertainties (the output noise and drift) will increase.

It should be noted that picoammeter manufacturers report 0.1% accuracy level for mA to μA input current measurements. This accuracy degrades to 0.3%–0.4% at nA currents. These values include one-year instabilities, percentage reading errors and offset values (usually given in current) and represent relative expanded ($k = 2$) uncertainties in the current-to-voltage conversion which are signal-gain dependent. These uncertainty values are about two decades higher than the relative expanded uncertainties reported here in table 2.

Based on the measurement results of the extended-gain reference (SDX) converter, low dc current routine calibrations can become a routine calibration service for national metrology institutes (NMIs). Also, current sources can be calibrated against the reference current-to-voltage converter and used as travelling standards to calibrate the signal gains of field-level current-to-voltage converters.

9. Conclusions

A reference current-to-voltage converter with extended-gain selections and improved electrical calibration was developed at NIST. It will enable measurements of low dc photocurrents from 1 nA to 100 μA with decreased uncertainty and traceability to NMI high-resistance measurements. The dc low-current measurements performed with the reference converter can reduce uncertainties of the same order of magnitude as the high-resistance measurements. The relative expanded uncertainties for the $10^7 \Omega$ to $10^9 \Omega$ calibrated feedback resistors range from 6×10^{-6} to 18×10^{-6} ($k = 2$) for optimal test conditions. The uncertainty of the $10^{10} \Omega$ feedback resistor calibration used in the highest gain is 50×10^{-6} ($k = 2$). The dc current measurement uncertainty of the reference converter at the 10^9 V A^{-1} gain is 55×10^{-6} ($k = 2$). This uncertainty propagates to the gain calibration of test current-to-voltage converters where 65×10^{-6} ($k = 2$) gain uncertainty can be obtained at 10^{10} V A^{-1} gain when the dc current is measured from a high output resistance current source. We estimate that the expanded uncertainties ($k = 2$) of commercial low-level dc current measurements of 0.1% (at 1 nA) could be reduced by more than a decade when utilizing the NIST converter design and calibration method. The uncertainty of the current-to-voltage conversion in commercial converters can be improved by $1\frac{1}{2}$ orders of magnitude when they are calibrated directly against the extended-gain (third-generation) reference converter using the substitution method. The internal (NIST) validation of the dc current measurement uncertainty of the reference converters has been made. The final total uncertainties of the NIST reference current-to-voltage converter measurements will need to include factors

such as temperature coefficient, voltage coefficient, long-term drift and transport effects. A high output resistance current source calibrated against the extended-gain reference converter is suggested for use as a travelling standard to calibrate signal gains of field current-to-voltage converters. Introduction of dc low-current routine calibrations in NMIs for the 1 nA to 100 μ A range is suggested here based on the improved (third-generation) reference current-to-voltage converter. With improved uncertainty low-current sources the 1 nA low end can be extended to either 100 pA or 10 pA.

Disclaimer

The mention of certain commercial products in this paper is for information purposes only and does not constitute an endorsement of the product by the authors or their institutions.

References

- [1] Gentile T R *et al* 1996 National Institute of Standards and Technology high-accuracy cryogenic radiometer *Appl. Opt.* **35** 1056–68
- [2] Brown S W, Eppeldauer G P and Lykke K R 2006 Facility for spectral irradiance and radiance responsivity calibrations using uniform sources (SIRCUS) *Appl. Opt.* **45** 8218–37
- [3] Kim W S *et al* 2008 A high precision calibration setup for low-current meters in the range of 10 pA to 1 fA *Conf. on Precision Electromagnetic Measurements (CPEM) (Broomfield, CO) Conference Digest* pp 358–9
- [4] Eppeldauer G 2000 Noise-optimized silicon radiometers *J. Res. Natl Inst. Stand. Technol.* **105** 209–19
- [5] Sipila P *et al* 2005 Calibration of current-to-voltage converters for radiometric applications at picoampere level *Proc. NEWRAD (Davos, Switzerland)* ed J Grober, pp 17–19
- [6] Eppeldauer G P 2009 Traceability of photocurrent measurements to electrical standards *MAPAN J. Metrol. Soc. India* **24** 193–202
- [7] Dziuba R F *et al* 1999 Fabrication of high value standard resistors *IEEE Trans. Instrum. Meas.* **48** 333–7
- [8] Jarrett D G 1997 Automated guarded bridge for calibration of multimegohm standard resistors from 10 M Ω to 1 T Ω *IEEE Trans. Instrum. Meas.* **46** 325–8
- [9] Elmquist R E *et al* 2004 NIST measurement service for dc standard resistors *NIST Technical Note* 1458
- [10] Graeme J G 1995 *Photodiode Amplifiers: Op Amp Solutions* (New York: McGraw-Hill) p 5